Nuclear Instruments and Methods in Physics Research A 816 (2016) 142–148

Contents lists available at ScienceDirect

Nuclear Instruments and Methods in Physics Research A

journal homepage: www.elsevier.com/locate/nima

A study of upward going particles with the Extreme Energy Events telescopes

M. Abbrescia [a,b], C. Avanzini [a,c], L. Baldini [a,c], R. Baldini Ferroli [a,d], G. Batignani [a,c], G. Bencivenni [d], E. Bossini [a,e], A. Chiavassa [f], C. Cicalo [a,g], L. Cifarelli [a,h], E. Coccia [i], A. Corvaglia [a,j], D. De Gruttola [a,k], S. De Pasquale [a,k], A. Di Giovanni [l], M. D'Incecco [l], M. Dreucci [d], F.L. Fabbri [d], E. Fattibene [m], A. Ferraro [m], R. Forster [n,o], V. Frolov [p], P. Galeotti [a,f], M. Garbini [a,h], G. Gemme [q], I. Gnesi [a,f], S. Grazzi [a,q], C. Gustavino [l], D. Hatzifotiadu [a,h,o], P. La Rocca [a,r], A. Maggiora [f], G. Maron [m], M.N. Mazziotta [s], S. Miozzi [a,d,i], R. Nania [a,h], F. Noferini [a,m], F. Nozzoli [i,t,*], M. Panareo [a,j], M.P. Panetta [a,j], R. Paoletti [a,e], L. Perasso [a,q], F. Pilo [a,c], G. Piragino [a,f], F. Riggi [a,r], G.C. Righini [a], A.R. Rodriguez [n,o], G. Sartorelli [a,h], E. Scapparone [h], M. Schioppa [a,u], A. Scribano [a,c], M. Selvi [h], S. Serci [f], E. Siddi [g], S. Squarcia [q], L. Stori [a,g], M. Taiuti [q], G. Terreni [c], M.C. Vistoli [m], L. Votano [l], M.C.S. Williams [e,o], S. Zani [m], A. Zichichi [a,h,o], R. Zuyeuski [a,o]

[a] Museo Storico della Fisica e Centro Studi e Ricerche E. Fermi, Roma, Italy
[b] INFN and Dipartimento di Fisica, Università di Bari, Bari, Italy
[c] INFN and Dipartimento di Fisica, Università di Pisa, Pisa, Italy
[d] INFN Laboratori Nazionali di Frascati, Frascati (RM), Italy
[e] INFN Gruppo Collegato di Siena and Dipartimento di Fisica, Università di Siena, Siena, Italy
[f] INFN and Dipartimento di Fisica, Università di Torino, Torino, Italy
[g] INFN and Dipartimento di Fisica, Università di Cagliari, Cagliari, Italy
[h] INFN and Dipartimento di Fisica, Università di Bologna, Bologna, Italy
[i] INFN and Dipartimento di Fisica, Università di Roma Tor Vergata, Roma, Italy
[j] INFN and Dipartimento di Matematica e Fisica, Università del Salento, Lecce, Italy
[k] INFN and Dipartimento di Fisica, Università di Salerno, Salerno, Italy
[l] INFN Laboratori Nazionali del Gran Sasso, Assergi (AQ), Italy
[m] INFN-CNAF, Bologna, Italy
[n] ICSC World Laboratory, Geneva, Switzerland
[o] CERN, Geneva, Switzerland
[p] JINR Joint Institute for Nuclear Research, Dubna, Russia
[q] INFN and Dipartimento di Fisica, Università di Genova, Genova, Italy
[r] INFN and Dipartimento di Fisica e Astronomia, Università di Catania, Catania, Italy
[s] INFN, sezione di Bari, Bari, Italy
[t] ASI Science Data Center, Roma, Italy
[u] Dipartimento di Fisica, Università della Calabria, Cosenza, Italy

ARTICLE INFO

Article history:
Received 29 January 2016
Accepted 31 January 2016
Available online 13 February 2016

Keywords:
Extreme Energy Events project
Cosmic muons
Muon decay

ABSTRACT

In this paper the first study of the upward going events detected by the telescopes of the Extreme Energy Event (EEE) project is reported. The EEE project consists of a detector array of Multigap Resistive Plate Chambers located at selected sites on the Italian territory. During autumn 2014 the first coordinated data taking period took place and around one billion candidate tracks were collected. Among them, of particular interest is the sample of particles which cross the telescopes from below. The results obtained demonstrate that the EEE telescopes can distinguish the electrons produced as decay products of cosmic muons stopped in the ground, or in the last chamber of the telescopes themselves, confirming the excellent performance of the system for the investigation of intriguing cosmic phenomena.

* Corresponding author at: ASI Science Data Center, Roma, Italy.
E-mail address: francesco.nozzoli@cern.ch (F. Nozzoli).

http://dx.doi.org/10.1016/j.nima.2016.01.090

1. Introduction

The Extreme Energy Events (EEE) project is an innovative experiment with the main goal of detecting the ground muon component of Extensive Atmospheric Showers (EAS)—particularly those generated by primaries with energy $>10^{19}$ eV [1,2].

The project started in 2004 and essentially consisted of building an array of about 50 telescopes scattered in the Italian territory and hosted in as many Italian high schools (plus two telescopes at INFN sections and two at CERN) [3]. Each station consists of three large area Multi-Gap Resistive Plate Chambers, very similar to the ones used for the time-of-flight system of the ALICE experiment at CERN, and therefore providing accurate particle tracking and timing information [4].

After its initial phase, the EEE collaboration has started a series of coordinated acquisition periods, during which data from all the active stations are collected, processed and analysed. The first period of coordinated data taking, hereafter *Pilot Run*, took place in October–November 2014. The data collected during the Pilot Run —~1 billion of candidate tracks in total—are now being analysed, with the purpose to continue, with a much improved statistics and monitored conditions, the analysis performed in the past years using limited time periods and sets of telescopes. In particular, events registered in coincidence at different sites are a direct measure of the EAS flux, and are thoroughly investigated [5-7]. Also, the variations of the cosmic muon rate at each telescope are interesting, since they can be correlated with astrophysical events such as, for instance, Forbush decreases [8].

Moreover, the study of events related to particles crossing the EEE telescope and directed from the ground upwards is intriguing. In principle, some of these events could be related to neutrinos crossing the Earth and interacting close to its surface just under the telescopes. In fact, these have been extensively investigated in the past [9]. Upward going events were also detected by the EEE telescopes, and their observation was reported elsewhere [10,11]. However, due to the rather limited statistics, it was not possible to draw definitive conclusions about their nature; however, from the beginning, it was clear that they were far too numerous to be interpreted just as events derived from neutrinos.

Here a more thorough analysis is reported, allowing the identification of the majority of the upward-going events as electrons produced by downward going muons crossing the telescope, but stopping in the material in the ground or in the telescope itself, where they decay. The fact that it was possible to discern these events among the billions collected in total is a clear indication of the excellent performance of the system during the whole Pilot Run.

2. The Extreme Energy Events project

The scientific multi-disciplinary value of the EEE project [3], its technical basis and its performance have been already described in [4,5,12,13]. Here, just a a synthetic description is presented.

2.1. Description of the telescopes

Each EEE telescope comprises three Multigap Resistive Plate Chambers (MRPCs), mounted horizontally on a metallic frame with vertical separation ranging between 0.4 and 1.0 m depending on the different stations.

An MRPCs consists of six gas gaps, as shown schematically in Fig. 1; the structure consists of two thicker glass plates (1.9 mm thick), coated with resistive paint, and five thinner glass plates (1.1 mm thick), spaced by 300 μm by means of commercial nylon

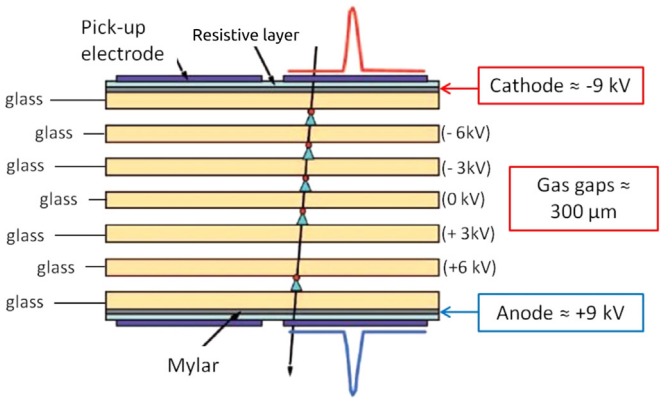

Fig. 1. Basic layout of a Multigap Resistive Plate Chamber used in the EEE telescopes.

fishing line; the glass volume resistivity is ~10^{13} Ωcm. Each MRPC features 24, 2.5 cm-wide, copper readout strips, separated from each other by 0.7 cm (i.e., a strip pitch of 3.2 cm) and an overall active area of 0.82×1.58 m^2; these readout strips are mounted on external fiberglass panels. The MRPCs are flushed with 98% of $C_2H_2F_4$ and 2% of SF_6 gas mixture. The chambers are operated in avalanche mode with a typical operating voltage around 18 kV supplied by DC/DC converters.

When an ionizing particle passes through the gas, it creates a number of primary ion-electron pairs, which exponentially grows in the avalanche process. Since the MRPCs glass plates have high resistivity, they act as dielectrics for the fast signal produced by the drift of the electrons in the gas avalanches. The induced signal, picked up by the copper strips, corresponds to all gas avalanches in all the gas. These signals are transmitted to the front-end boards (FEA) mounted at the two ends of the chamber.

The signals coming from the FEAs on each telescope are processed by a trigger card in order to provide information to the VME-based data acquisition. A six-fold coincidence of both front-end cards of the three MRPCs generates the data acquisition trigger. The particle impact point is determined by the position of the hit strip in one direction; in the other direction the difference of signal arrival time at the strip ends, measured by two multi-hit TDCs (CAEN Mod. V1190A/B), localizes the position along the lenght of the strip. At the operating voltage, the measured MRPC efficiency is typically 95%. The TDCs are operated with a 100 ps bin width, so that strip dimension and time difference provide an overall spatial resolution of about 1 cm along the two coordinates.

The absolute time of each event is recorded and synchronized by means of Global Positioning System modules, in order to get the event time stamp and to correlate the information collected by different telescopes. The data acquisition is controlled by a LabView program running on a PC connected to the VME crate via an USB-VME bridge. A picture of one of the EEE stations selected for the analysis described in this work is shown in Fig. 2.

2.2. Data processing and data quality monitoring

The data-processing infrastructure for the EEE experiment is provided by CNAF (*Centro Nazionale Analisi Fotogrammi*), the central computer facility of the Italian National Institute for Nuclear Physics (INFN) and one of most prominent centers for distributed computing in Italy.

The data acquisition is organized in units (or *runs*) of 50,000 events each, corresponding to 15–30 min of data taking, depending on the acceptance of the telescope. During periods of coordinated data acquisition, the DAQ systems are running continuously under the direct supervision of the students and professors. Data from each school

participating in the project are automatically transferred to CNAF and processed in almost real time on a dedicated machine. For each run the standard event reconstruction (see Section 2.3) is performed and a data summary tape (DST) in ROOT [14] format is created for calibration and scientific analysis purposes. All the book-keeping is performed via a dedicated MySql database.

Run-by-run and daily summary reports are also automatically produced for each telescope and made available through a central web interface by the data-processing pipeline. They constitute one of the main data quality monitoring resources for the shifters and the run coordinators.

2.3. Event reconstruction

The first step of the event reconstruction is a clustering stage, where hits in the detector that are contiguous to each other are grouped into clusters. The average cluster multiplicity for typical atmospheric-muon events is low: one cluster per plane for the majority of the events.

We feed the cluster coordinates into two independent unweighted linear fits to triplets of points in the two orthogonal x–z and y–z views (see Fig. 3 for an event display). The two fits are then combined to provide the best-fit track parameters, i.e., the direction cosines and the track intercept with the middle MRPC plane. We define the square root $\bar{d}$ of the quadratic sum of the three-dimensional distances d_i between the cluster positions and the best-fit track

$$\bar{d} = \left(\sum_{i=1}^{3} d_i^2 \right)^{\frac{1}{2}} \tag{1}$$

and use it as an indicator of the fit quality (the index i in the sum is running over the three MRPC planes). When the cluster multiplicity in one or more planes is greater than 1, all the possible triplets of points are fitted and the track with the lowest $\bar{d}$ is used in the analysis. The $\bar{d}$ value for the best track can amount to several cm for low-energy particles, and in the remaining of this work we do require events to have $\bar{d} < 10$ cm in order to be included in the analysis. We anticipate, however, that our conclusions are largely independent from the precise choice of the cut value.

The time of flight T_f of each event is measured as the time difference between the hits in the uppermost and lowermost MRPC plane. These two planes are physically fed into the same time-to-digital converter and the resolution on the time of flight is of the order of a few hundreds of ps or better. For a typical track length l~1 m (or T_f~3 ns), this translates into a relative error on the measurement of the velocity

$$\beta = \frac{v}{c} = \frac{l}{cT_f} \tag{2}$$

of ~10% for an ultra-relativistic particle. We conventionally assign positive β values to downward-going particles and negative β values to upward-going particles.

Fig. 2. Picture of the EEE station FRAS-02, located in the high school *ITT Enrico Fermi*, Frascati (close to Rome). All the basic components of the detectors and the associated data acquisition system are shown: the MRPCs, the VME crate, the low- and high-voltage supply systems, the computer controlling the DAQ and the gas cabinet in the background.

3. Data analysis

The data sample used for this analysis is a subset of the events acquired in the EEE Pilot Run, spanning the ~3-week time interval between October 21 and November 14, 2014. In total, 22 telescopes were active for at least part of the pilot run; 813,246,560 events were observed in 26,418 data taking runs where 657,441,238 candidate tracks were analysed. We selected events from three representative telescopes that featured stable operation with a ~100% duty cycle through the entire pilot run:

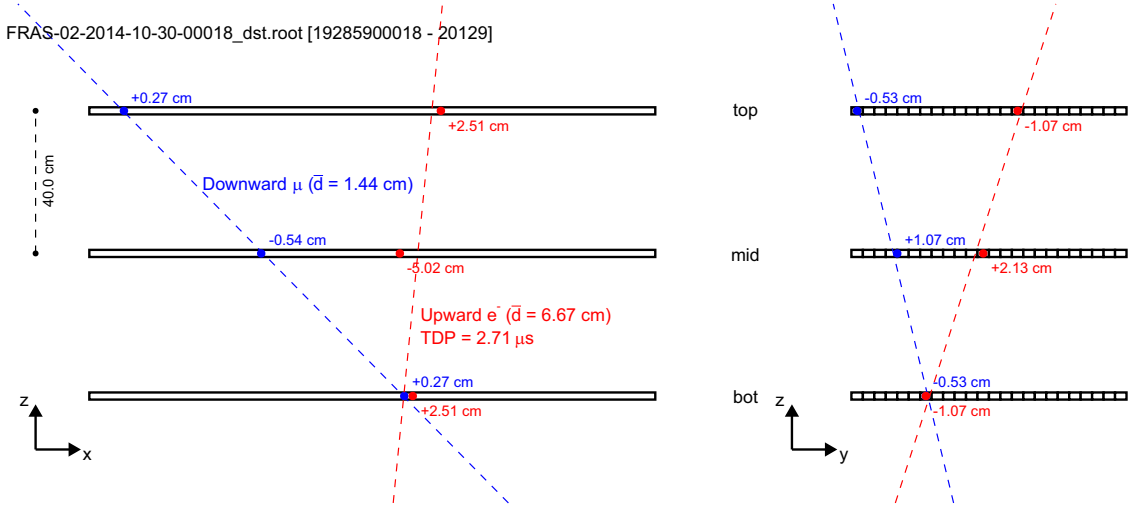

Fig. 3. Event display of two tracks, separated in time by ~2.7 μs, acquired during the pilot run—a downward-going candidate muon (in blue) and an upward-going candidate electron (in red). Though, due to the multiple Coulomb scattering, it is only possible to constrain the vertex position to a few cm, we found, in this case, a vertex position consistent with the lowermost MRPC chamber. We note that the $\bar{d}$ is significantly larger for the upward-going particle than for the downward-going one. (The dots indicate the positions of the clusters in the two views, the dotted lines are the best-fit tracks and the numbers close to the hits represent the spatial residuals.) (For interpretation of the references to color in this figure caption, the reader is referred to the web version of this paper.)

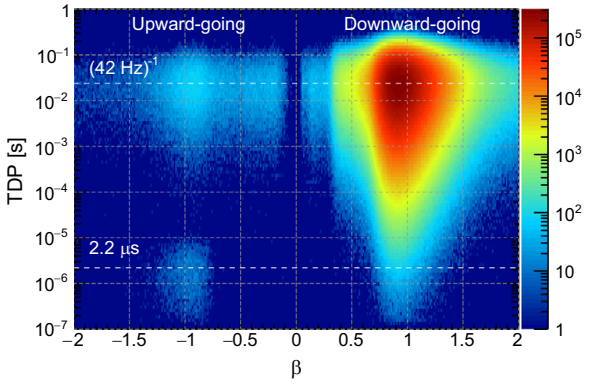

Fig. 4. Distribution of our event sample in the TDP (time difference to previous event)-β plane. Positive (negative) β values correspond to downward (upward)-going events. The average data acquisition rate for the telescopes used in this study is ~42 Hz (see Table 1), corresponding to an average TDP ~24 ms.

1. FRAS-02 (located in the high school "*ITT Enrico Fermi*", Frascati, close to Rome).
2. SAVO-01 (located in the high school "*Liceo Scientifico Orazio Grassi*", Savona).
3. SAVO-02 (located in the high school "*Liceo Chiabrera-Martini*", Savona).

3.1. Upward going events

Out of the ~1.3×10^8 events with a good reconstructed track ($\bar{d} < 10$ cm) in the original sample, about 7×10^4 (or almost one in a thousand) feature a negative β, i.e., they are upward-going. While a direct comparison with other measurements, e.g., by MACRO [9], is not trivial due to the different muon energy thresholds, this is much larger than the expected contribution from atmospheric/extraterrestrial neutrino. The calculation in [15,16], for example, provides an estimate for muons from atmospheric neutrinos of the order of 10^{-13} s^{-1} cm^{-2} sr^{-1}, which, when multiplied by the typical acceptance of an EEE telescope, translates into something of the order of ~1 observed event every 10 years. This is one of the motivations that prompted us to investigate the origin of this large number of events.

The working hypothesis at the base of our analysis is that a significant fraction of the upward-going events is actually originating from downward-going muons which range out in the lowermost MRPC assembly or in the concrete immediately below the telescope where they stop and subsequently decay at rest into

$$\mu^{\pm} \rightarrow e^{\pm} + \nu_{e/\mu} + \bar{\nu}_{\mu/e}.$$

The two neutrinos produced in the muon beta decay would then travel undetected, while the outgoing electron could occasionally escape the concrete and traverse the three chambers, triggering the telescope.

A schematic representation of the process is shown in Fig. 3 through an actual event display collected during the pilot run.

The basic signatures are:

1. the temporal separation between the downward-going (parent) muon and the upward-going (daughter) electron should be of the order of the muon lifetime (~2 μs);
2. the β of the parent muon should be small enough for it to range out near to the surface of the concrete underneath the telescope, or in the lowest chamber of the telescope;
3. accordingly, the $\bar{d}$ of the reconstructed track from the parent muon should be relatively large, due to multiple Coulomb scattering;
4. similarly, the $\bar{d}$ of the reconstructed track from the upward-going (low-energy) electron should be much larger than that of the parent muon.

In order to confirm our working hypothesis, each of these signatures has been thoroughly studied as described in the following sections.

Finally, it is worth to note that while positive muons can only decay freely, negative muons have another disappearance channel in matter, which is muon capture by a nucleus (as for electrons). The negative muon can spend some time inside the nucleus, and has a sizeable (Z-dependent [17]) probability to be captured by a proton in the nucleus. Therefore, since negative muons in matter can either decay or be captured, their lifetime in matter is different (and smaller) from that of positive muons. This is extensively discussed e.g., in [18,19]. Thus we expect a small difference in the measured muon lifetime value with respect to the tabulated lifetime of the muon at rest that is related to the atmospheric muon charge ratio μ^+/μ^-. The muon charge ratio value is about 1.3 at sea level and reflects the excess of π^+ (K^+) over π^- (K^-) in the forward fragmentation region of proton-initiated showers together with the fact that there are more protons than neutrons in the primary spectrum [20–22].

3.2. Temporal analysis

In Fig. 4, the time difference with respect to the previous event (which we shall refer to as TDP hereafter) is plotted for our sample as a function of the measured particle velocity $\beta = v/c$. While the core of the distribution is centered around β~1 and TDP ~24 ms (i.e., is compatible with downward-going relativistic muons produced by atmospheric showers and impinging on the detector at an average rate of ~42 Hz), two separate populations of upward-going relativistic particles (with β close to −1) are clearly visible, one of which is characterized by a TDP of the order of μs, i.e., much smaller than the inverse of the average data acquisition rate. As mentioned before, the latter population accounts for some ~4×10^{-5} of the total number of events in our sample.

In order to investigate the parent–daughter scenario outlined at the beginning of this section, in Fig. 5 we restrict ourselves to the negative-β half-plane (that is, upward-going particles) and we plot the TDP as a function of the measured velocity of the *previous* event—i.e., the putative parent. It is clear that the small population of upward-going events with TDP ~μs in Fig. 4 is in a parent–daughter relationship with relatively slow down-going particles with $0.5 < \beta < 0.8$.

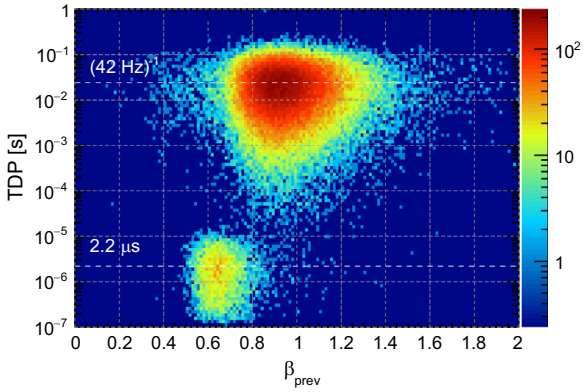

Fig. 5. Distribution of the TDP for our upward-going event sample (negative-β half-plane in Fig. 4) as a function of the measured β of the previous event (i.e., the putative parent). Note that the left half-plane is not shown, as the vast majority of the parent particles are downward-going.

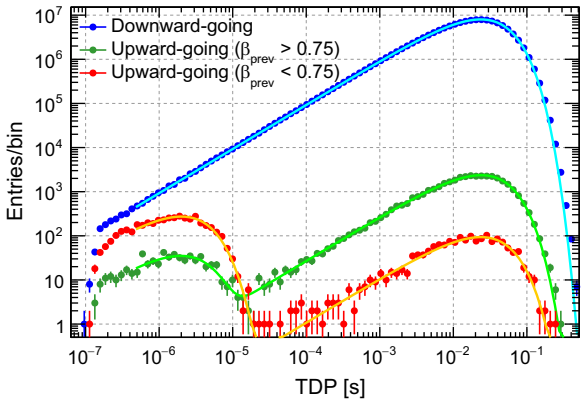

Fig. 6. Distribution of the time difference with respect to the previous event for three different classes of relativistic ($0.75 < |\beta| < 1.3$) particles: downward-going events (blue), upward-going events following a fast ($\beta_{prev} > 0.75$) downward-going track (green), and upward-going events following a slow ($\beta_{prev} < 0.75$) downward-going track (red). The sharp cutoff feature around 150 ns is due to the dead time of the data acquisition system. (For interpretation of the references to color in this figure caption, the reader is referred to the web version of this paper.)

Assuming that these slow particles are indeed low-energy atmospheric muons, for β~0.65, we estimate a range in Al or in concrete of the order of 2–3 cm [23]. The energy distribution of the Michel electrons emitted in the muon decay peaks at ~45 MeV, corresponding to an electron range of ~7 cm, i.e., larger than that of the parent muon [24]. This would allow the daughter electron to escape the absorbing material underneath the telescope, and potentially trigger the telescope itself.[1]

We stress that, although we can *directly* identify this parent–daughter relationship in a small sub-population only (~4×10^{-5} of the total sample, or ~6% of the upward-going events), it is not unlikely that most (or all) of the remaining upward-going particles could be electrons from the beta decay of muons being absorbed in the vicinity of the lowest chamber without triggering the telescope. This will be investigated in more detail in the next section.

In order to measure the lifetime of the decay process we plot the TDP distribution for several classes of events (downward-going relativistic particles, upward-going relativistic particles following a fast downward-going one, and upward-going relativistic particles following a slow downward-going one) in Fig. 6. We note that, when logarithmically binned, the distribution of time differences between successive events for a Poisson process with time constant τ is bell-shaped[2] with a maximum at TDP = τ. The representation in Fig. 6 is therefore very effective in visually highlighting the presence of different exponentially-distributed temporal components.

The continuous lines in Fig. 6 represent the exponential (for downward-going particles) and double-exponential (for upward-going particles) models that best fit the data. For the two populations of upward-going events, the fast and slow temporal components of the double exponential are meant to capture the delayed coincidences induced by the muon decay and the standard underlying Poisson process dictated by the rate of data acquisition, respectively. We note that, as already stated before, the vast majority of upward-going tracks following a slow downward-going particle is related to muon decays. Table 1 summarizes the fit parameters. We note that our estimate for the time constant of the delayed coincidences in Table 1 (2.04 ± 0.04 μs) is ~10% smaller than the tabulated lifetime of the muon at rest. This is related to the well-known matter effects for stopping negative muons, as studied already, e.g., in [18,19] and discussed in Section 3.1 due to the atmospheric muon charge ratio μ^+/μ^-.

[1] By taking into account the material budget of the three chambers, a minimum energy for the electrons to trigger the telescope of ~25 MeV can be estimated.

[2] Formally, if t is exponentially distributed ($dN/dt = N_0 e^{-t/\tau}$), then the probability density function of the variable $x = \log_{10}(t)$ is given by:

$$\frac{dN}{dx} = N_0 \ln(10) \times 10^x e^{-10^x/\tau}.$$

Table 1
Best-fit parameters for the models shown in Fig. 6. Note that we quote the time constant for the fast components (which is germane to the muon lifetime) and the inverse of the time constant for the slow components—which indicates the average data acquisition rate.

Population	τ_{fast} [μs]	$1/\tau_{slow}$ [Hz]
Downward-going	–	42.502 ± 0.004
Upward-going ($\beta_{prev} > 0.75$)	1.95 ± 0.10	41.98 ± 0.22
Upward-going ($\beta_{prev} < 0.75$)	2.01 ± 0.04	42.3 ± 1.1

3.3. Particle identification

Due to their different mass and typical energy, electrons from muon beta decay and relativistic muons experience significantly different multiple scattering when crossing the detector material. For reference, given an overall thickness of ~20%X_0 for a single detection-plane assembly, a vertical 45 MeV electron will be scattered with an average angle of ~7° in Gaussian approximation, whereas the same figure is of the order of ~0.3° for a 1 GeV muon. When extrapolated to the typical lever arm between planes (~50 cm), this translates into a linear displacement of ~6 cm and a few mm, respectively—i.e., the electron can be deflected by ~2 times the strip pitch, while at the given detector resolution the muon essentially travels in a straight line. This potentially allows a statistical identification of electron events using $\bar{d}$ as a discriminator.

Based on these considerations we define a simple track shape indicator ξ as

$$\xi = \log_{10}(1 + \bar{d}). \quad (3)$$

In Fig. 7 this shape indicator is plotted as a function of β for three classes of events:

1. the entire sample, i.e. mainly fast downward-going muons, with a small contribution from the upward-going events under investigation (top panel);
2. a clean electron sample, obtained selecting upward-going tracks following a slow downward-going muon by <30 μs (lower-left panel).
3. a clean slow-muon sample, obtained selecting downward-going particles followed by an upward-going particle within less than 30 μs (lower-right panel)

The mean value of the shape indicator for upward-going electrons is ξ~0.85 (corresponding to a $\bar{d}$~6 cm), which, as expected, is much larger than the mean value (ξ~0.5, corresponding to a $\bar{d}$~2 cm) for the relativistic downward-going muons. We also note that the average value of the shape indicator for slow muons (ξ~0.6, or $\bar{d}$~3 cm) is slightly larger than the corresponding figure for fast muons. This is also expected, since the average multiple-scattering angle for a muon with $\beta = 0.65$ (kinetic energy ~35 MeV) is of the order of 5°.

As pointed out at the beginning of this section, the differences in the shape indicator can be used to infer the relative abundance of the different upward-going populations via a template fitting.

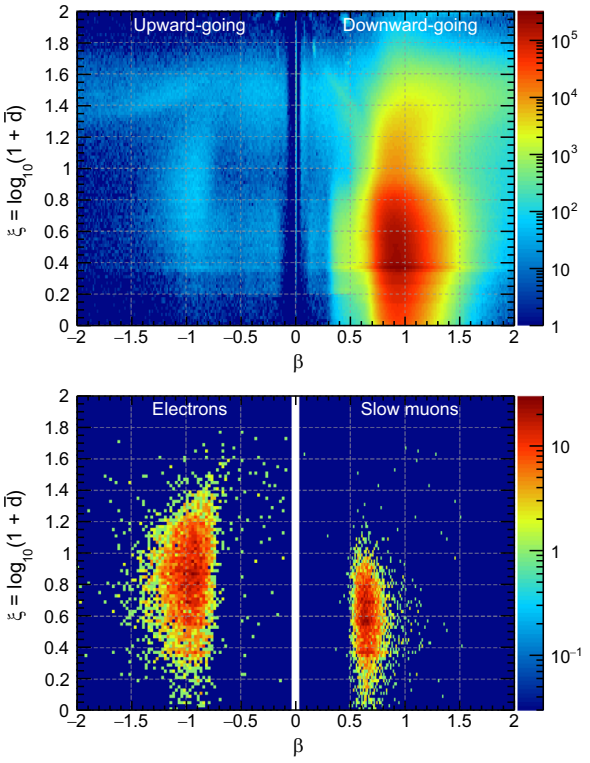

Fig. 7. Distribution of the shape indicator $\xi = \log_{10}(1 + \bar{d})$ as a function of the particle velocity β for all the events (top panel) and for our control samples of electrons (lower-left panel) and slow muons (lower-right panel).

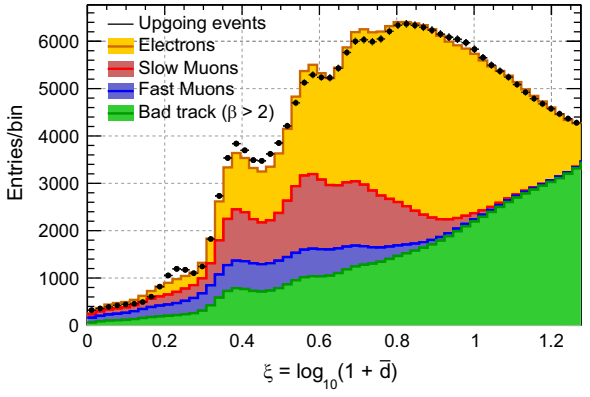

Fig. 8. Example of template fit to the various upward-going populations using our shape indicator as a discriminating variable. While the exact abundances of the sub-dominant components depend, to some extent, on the exact prescription we use to extract the corresponding templates, the electron component is always dominant. The various peaks in the distributions are due to the digitizing induced by the relatively large pitch of the strips.

More specifically, we derive from the actual data template distributions for fast muons, slow muons and electrons. In order to account for the background induced by misreconstructed events, peaking at large ξ values, we derive a template using the side bands $|\beta| > 2$. This is shown qualitatively in Fig. 8.

It should be noted that the templates are partially degenerate with each other, and therefore it is not trivial to assess the systematic uncertainties associated to our measurement. Nonetheless, while the relative abundances of the sub-dominant populations show some (weak) dependence on the cuts defining the templates, the fact that the electron component is the dominant one is a very important result. This provides compelling evidence that, even if the timing analysis only allows us to identify the muon decay as the underlying mechanism for a relatively small upward-going population, electrons from muon decay indeed account for most of the upward-going events in our sample.

A detailed study of the other sub-dominant components (e.g., upward-going back-scattered muons) would require a significant amount of additional analysis and will be addressed in a future work.

4. Conclusions

The origin of the upward-going events observed by the EEE telescopes is one of the most important purposes of the EEE project. The first step is to study those events which do simulate the genuine upgoing events. In fact relativistic upgoing electrons are produced from the decay of downward-going muons stopping in the lowermost part of the telescope or in the ground immediately below it. For about 6% of the sample, the downward-going parent muon triggers the telescope and can be tagged.

Being able to perform such an analysis is a clear indication of the excellent performance of the EEE network and its telescopes. This is relevant for the measurements about coincidences, cosmic rays variations, etc. that are at present ongoing. Moreover these measurements have a clear value from the educative point of view, which is one of the goals of the EEE experiment.

After the Pilot Run, the Run1 of the EEE experiment took place. This lasted from February 23 up to April 30, 2015, and four billion events have been collected, which are currently being reconstructed and analysed. The analysis described here with a much larger data sample represents the next step for the EEE project. Moreover, improvements in the reconstruction procedure have included additional information with respect to this analysis, such as the vertexes of the capture/decay and a second track in the same event. This will lead to an even more refined analysis in the future.

Acknowledgments

Nothing of what has been described here would have been possible without the hard work, passion, and dedication of all the students and teachers involved in the EEE Project. To them all goes the warm acknowledgement of the whole EEE scientific community.

References

[1] Centro Fermi web site: ⟨http://www.centrofermi.it/eee⟩.
[2] R. Antolini, et al. (EEE collaboration), The EEE project, in: 29th ICRC Proceedings, vol. 8, 2005, p. 279.
[3] A. Zichichi, Progetto "La Scienza nelle Scuole"—EEE: Extreme Energy Events, Società Italiana di Fisica, Bologna, 2004.
[4] A. Akindinov, et al., Nuclear Instruments and Methods in Physics Research Section A 456 (2000) 16.
[5] M. Abbrescia, et al., (EEE collaboration), European Physical Journal Plus 128 (2013) 148.
[6] M. Abbrescia, et al., (EEE collaboration), European Physical Journal Plus 129 (2014) 166.
[7] M. Abbrescia, et al., (EEE collaboration), Nuovo Cimento B 125 (2010) 243.
[8] M. Abbrescia, et al., (EEE collaboration), European Physical Journal Plus 126 (2011) 61.
[9] M. Ambrosio, et al., (MACRO collaboration), Physics Letters B 434 (3–4) (1998) 451.
[10] M. Abbrescia, et al., (EEE collaboration), European Physical Journal Plus 128 (2013) 62.
[11] G. Piragino, Giornale Di Fisica 51 (2010) 295.
[12] M. Abbrescia, et al., (EEE collaboration), Nuclear Instruments and Methods in Physics Research Section A 593 (2008) 263.

[13] M. Abbrescia, et al., (EEE collaboration), Nuclear Instruments and Methods in Physics Research Section A 588 (2008).
[14] R. Brun, F. Rademakers, Nuclear Instruments and Methods in Physics Research Section A 389 (1997) 81, See also ⟨http://root.cern.ch/⟩.
[15] J.W. Elbert, M. Iacovacci, V. Silvestrini, Europhysics Letters 14 (1991) 181.
[16] T.K. Gaisser, et al., Physical Review D 30 (1984) 985.
[17] V. Gilinsky, J. Mathews, Physical Review 120 (1960) 1450.
[18] B. Rossi, High Energy Particles, Prentice Hall, New York, 1952.
[19] A. Grossheim, et al., Physical Review D 80 (2009) 052012.
[20] M. Boezio, et al., Physical Review D 62 (2000) 032007.
[21] S. Haino, et al., (BESS Collababoration), Physics Letters B 594 (2004) 35.
[22] P. Adamson, et al., (MINOS collaboration), Physical Review D 76 (2007) 052003.
[23] D.E. Groom, N.V. Mokhov, S. Striganov, Atomic Data and Nuclear Data Tables 78 (July (2)) (2001).
[24] M.J. Berger, J.S. Coursey, M.A. Zucker, J. Chang, 2005, ESTAR, PSTAR, and ASTAR: computer programs for calculating stopping-power and range tables for electrons, protons, and helium ions (version 1.2.3), National Institute of Standards and Technology, Gaithersburg, MD. (Online) Available: ⟨http://physics.nist.govStar⟩, 2015.